MAGNITUDE ESTIMATION FOR EARTHQUAKE EARLY WARNING (EEW) FOR EASTERN CAIRO AND THE SOUTH OF SINAI

Ibrahim Zahra* **Supervisor: Bunichiro SHIBAZAKI****
MEE17702

ABSTRACT

In this study, we examined 3 techniques of magnitude estimation for earthquake early warning (EEW): corner period τ_c, peak predominant period τ_{max}^{p} and initial peak displacement P_d. We established the best fit relation between each of these parameters and magnitude. We also examined real-time parameters like the filter cut-off frequency and the time-window of estimation in order to find the values that give the best fit relation in each technique. We chose eastern Cairo and the South of Sinai because of its high importance in Egypt's economy and future urbanization as well as the moderate to high seismic activity in this region. We used a dataset of 20 earthquakes between 1999 and 2015, from the Egyptian National Seismic Network catalog, in the target region. All of the selected events, except for one, have local magnitude over 4.0. The results of τ_c and τ_{max}^{p} show that the error in magnitude estimation could reach up to 1.0, in this dataset. The results also indicate that P_d is the best parameter for magnitude estimation in EEW. Based on results, we made recommendations that could be extended into the action plan required to achieve an EEW system in Egypt.

Keywords: Earthquake early warning (EEW), Corner period τ_c, Peak predominant period τ_{max}^{p}, Initial peak displacement P_d

1. INTRODUCTION

Rapid magnitude estimation is a critical task for earthquake early warning (EEW) systems because EEW utilizes the few seconds between the P-wave and damaging S-waves or surface waves to minimize the damage. The magnitude estimation methods in EEW can be categorized into two categories: methods use time-domain parameters like initial peak displacement, and frequency-domain parameters like corner period τ_c or peak predominant period τ_{max}^{p}. All these parameters should be determined in the first few seconds from the P-wave onset.

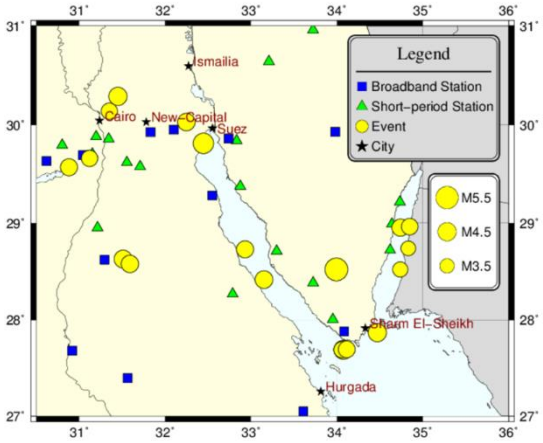

Figure 1. The selected region, events and ENSN stations.

The purpose of this study is to determine which is the best parameter that can be used for magnitude estimation and establish the relationship between the magnitude and each of these parameters, which could be used in the EEW system. Also, we would determine the best processing parameters that give the best results such as the usage of filters and the time-window of measurement as well as testing the usability of short-period data after making a simplified instrumental correction that can be applied in real-time for EEW purpose.

*National Research Institute of Astronomy and Geophysics (NRIAG), Egypt.
**International Institute of Seismology and Earthquake Engineering, Building Research Institute, Japan.

2. STUDY AREA AND DATA SELECTION

The target area, in Figure 1, is eastern Cairo and the South of Sinai, which is very important for Egypt's economy and in urban development. Many new cities were established in this area in the past 20 years, which have millions of inhabitants, along the highways connecting Cairo to Suez and Ismailia. Moreover, a few new cities under establishment like the new capital city in Egypt's vision for 2030. The future projects contain high rise buildings and high-speed train in addition to a suspension bridge connecting Egypt and Saudi Arabia over the Gulf of Aqaba. The target area also was selected because of its seismic activity because of the plate boundary along the Red Sea.

The selected dataset, in Figure 1, contains 20 events from the Egyptian National Seismic Network (ENSN) of local magnitude over 4.0, except for one M3.7 to enhance regression analysis. The events occurred between 1999 and 2015. While the largest event recorded in the study was of magnitude 7.2 in 1995 in the Gulf of Aqaba, unfortunately, we do not have local data available because ENSN was established in 1997. The events were selected based on data availability limitations. Some parameter estimation requires using only broadband data and other parameters require limited epicentral distance between the station and the events. Also, all the selected events exist in one or more of these international catalogs: USGS, IRIS, ISC and EMSC catalogs, because the magnitude determined in the ENSN catalog was inconsistent with the results of some events.

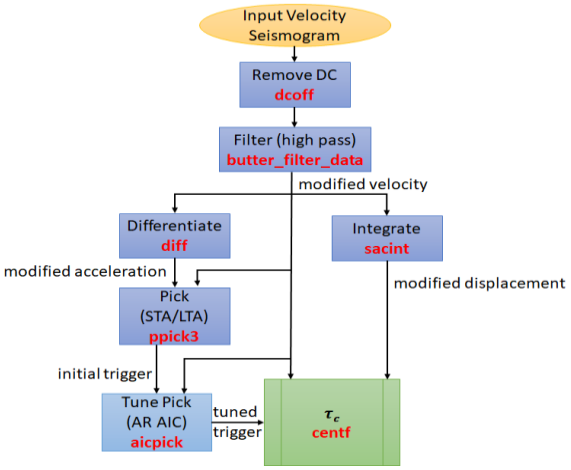

Figure 2. A simplified flowchart of Dr. Yamada's program for calculating τ_c (Yamada and Mori, 2009).

3. THEORY AND METHODOLOGY

3.1. Corner period τ_c

We used the program provided by Dr. Yamada (Yamada and Mori, 2009) for determining τ_c. The simplified flow chart of Figure 2 shows explains how it works. First, we input a velocity record, remove the mean (dcoff), filter the data (butter_filter_data) using Butterworth high pass filter to obtain modified velocity, integrate (sacint) and differentiate (diff) to obtain modified displacement and modified acceleration, respectively. Modified velocity and acceleration are used in picking (ppick3) using Allen (1978) STA/LTA method, and then the picking is tuned for more accuracy (aicpick) using AR-AIC (Takanami and Kitagawa, 1988). The modified velocity and displacement are used to calculate τ_c (centf) according to Kanamori (2005): $\tau_c = 2\pi / \sqrt{\int_0^{\tau_0} \dot{u}^2(t)dt \,/ \int_0^{\tau_0} u^2(t)dt}$, where $u(t)$ is the modified displacement, $\dot{u}(t)$ is the modified velocity and τ_0 is the selected time-window of measurement.

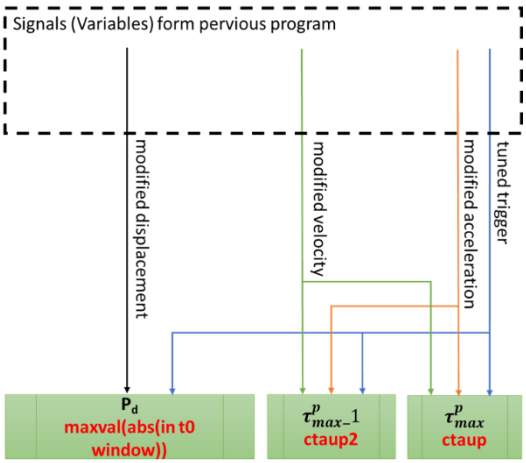

Figure 3. Modification to the program to compute P_d and τ^p_{max}, where τ^p_{max}_1 is a a modified version by Shieh *et al.* (2008).

3.2. Maximum predominant period τ^p_{max} and initial peak displacement P_d

We modified the previous program to obtain τ_{max}^{p} and P_d, as shown in Figure 3 We used the same modified displacement to calculate P_d, which is the absolute maximum displacement in the selected t0 time window from the P-wave onset. Then, P_d value should be converted into physical units like cm or m to be used in magnitude estimation.

Both modified velocity and acceleration are used to calculate τ_{max}^{p} and $\tau_{max}^{p}\_1$. τ_{max}^{p} is calculated after Allen and Kanamori (2003). First calculate the predominant period τ_i^p at each sample: $\tau_i^p = 2\pi\sqrt{X_i/D_i}$, where i is the sample number, $X_i = \alpha X_{i-1} + x_i^2$, where x_i is the modified velocity, $D_i = \alpha D_{i-1} + (dx_i/dt)_i^2$, where $(dx_i/dt)_i$ is the modified acceleration, and $\alpha = 1 - dt$ is a smoothing factor where dt is the sampling interval. Then, τ_{max}^{p} is the maximum of τ_i^p in the specific time window. $\tau_{max}^{p}\_1$ is the same as τ_{max}^{p} except for setting the first 0.05 s of τ_i^p to zero, to stabilize the values of τ_{max}^{p} (Shieh *et al.*, 2008).

3.2. Short-period instrumental correction

We have written a new subroutine to correct the response of short-period seismograms following the 3 stage filtering proposed by Yamada *et al.* (2014). The suggested correction was for enabling the usage of the high-sensitivity network (Hi-Net) short-period stations, to be used in the JMA EEW system. JMA is currently using their own strong-motion network, which is not as dense as Hi-Net, for EEW system, to calculate P_d. Figure 4 shows the amplitude response of each stage.

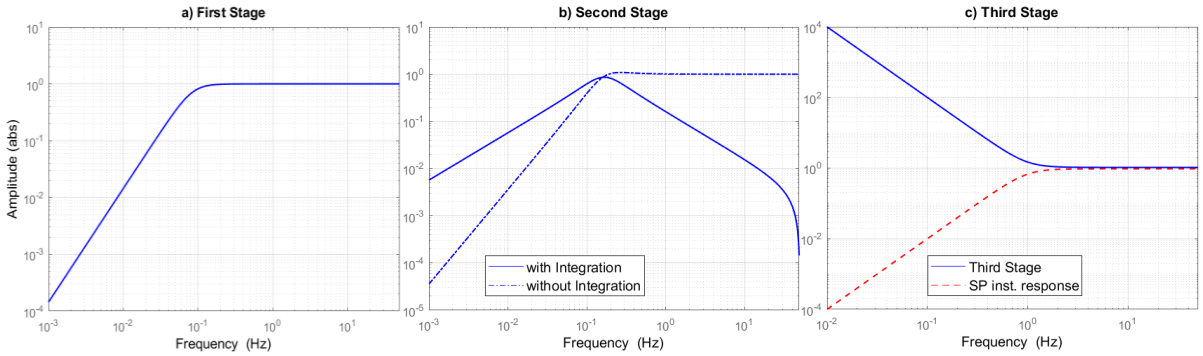

Figure 4. Amplitude response of each stage: a) is a 12 s (0.083 Hz) HPF, b) is a 6 s HPF with integrator (solid-line) and without integrator (dashed-line), and c) is a simplified instrument correction (solid-line) which is the inverse response of a short-period seismometer with a natural period of 1 s.

The reason behind using 3 stages is that P_d tends to saturate in short-period seismograms especially for large earthquakes because the long period waves that are radiated by these earthquakes are heavily damped by short-period seismometers. The first stage is a 12 s high pass filter (HPF) which should limit the noise waves longer than 12 s because it would be amplified after the instrument correction. The second stage, 6 s HPF, is the main filter used by JMA (Katsumata, 2008) except for having single integrator to convert velocity to displacement, while JMA EEW system uses double integration to convert acceleration to displacement. The third stage is a simplified instrumental correction (Zhu, 2003), which has the opposite response of a short-period seismogram with 1 s natural period. We shall extend this method to calculate τ_c and τ_{max}^{p} using short-period seismograms. In such case, to obtain corrected velocity, 2nd stage should not include integration.

4. RESULTS AND DISCUSSION

4.1. Corner period τ_c

Using only broadband data, we find the best fit relationship between log(τ_c) and the magnitude. We tested the relation between different combinations of filter cut-off period (5, 6 or 13 s) and time-window (2, 3 or 4 s). For each combination, we determined the linear relation using magnitudes from the local catalog or using average magnitudes among international catalogs. The results always were better in case of the average of international catalogs' magnitudes. That is shown in Figure 5 in terms of the standard error (SDE) and the scattering. We also tried using short-period data after instrumental correction but the resulted values of τ_c were almost constant regardless of the magnitude. The best results were obtained using 5 s high pass filter and 4 s time window, and the best linear relation was:

$$M = 0.585 \times log(\tau_c) + 4.438 \quad (1)$$

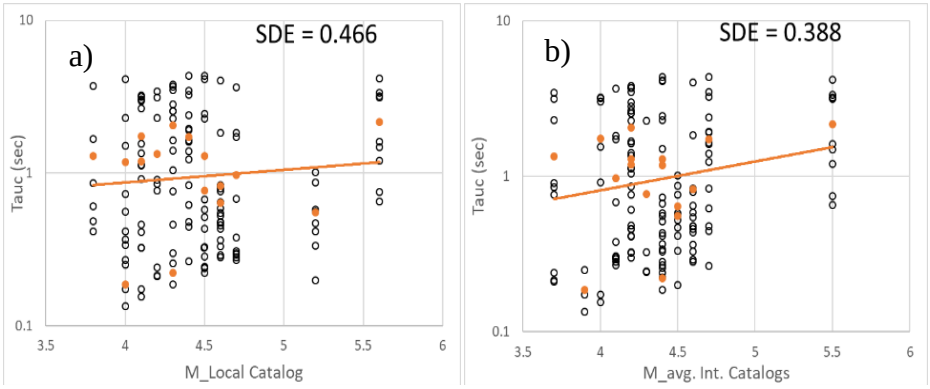

Figure 6. τ_c vs. magnitude: a) From the ENSN local catalog, b) average of International catalogs' magnitudes. Open circles are single station value and closed circle is the average value for one event.

4.2. Maximum predominant period τ_{max}^{p}

Using broadband data only, in Figure 6 (a), we could not obtain a linear relationship between τ_{max}^{p} and the magnitude. We tried the corrected short-period data and the results became better, except for some values of τ_{max}^{p} that were almost constant at 0.031 or 0.061 s, as shown in the bottom of in Figure 6 (b). When we limited the epicentral distance to ≤ 250 km between the event and the station, these small values disappeared and we obtained the linear relationship in Figure 7.

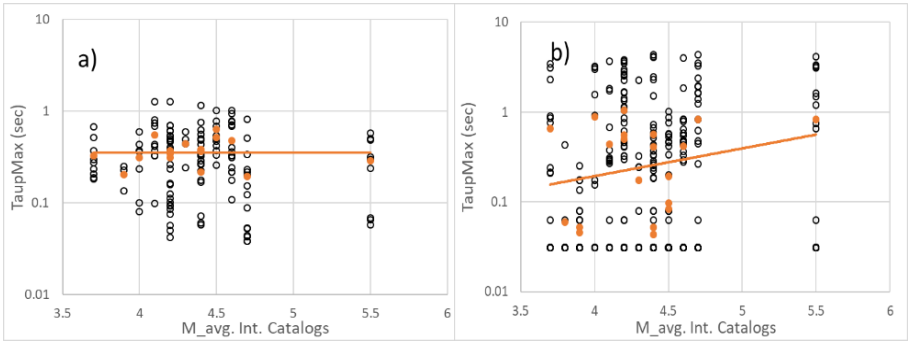

Figure 5. τ_{max}^{p} vs. magnitude: a) broadband data only, b) broadband + corrected short-period. Small constant values around 0.03 s and 0.06 s are shown in b).

As we explained with τ_c, we tested the magnitude from the local catalog and the average magnitude of international catalogs. We found the average magnitude has a better linear relation with τ_{max}^{p}, exactly the same as τ_c. We tested the same combinations of filter and time-window, and found the best relation using both broadband and corrected short-period data, filtered by 5 s HPF and 2 s time-window (which is shown in Figure 7):

$$M = 0.593 \times log(\tau_{max}^{p}) + 4.203 \quad (2)$$

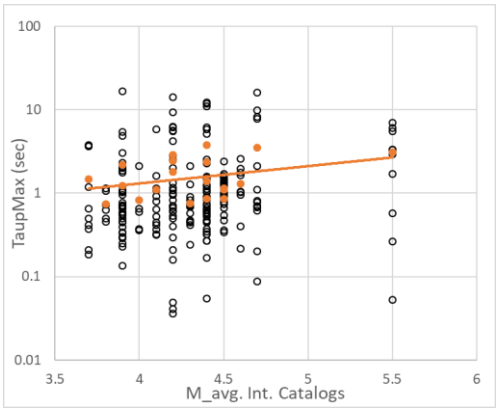

Figure 7. Best results of τ_{max}^{p} vs. M using broadband + corrected short-period data with 5 s HPF and 2 s time-window.

4.3. Initial peak displacement P_d

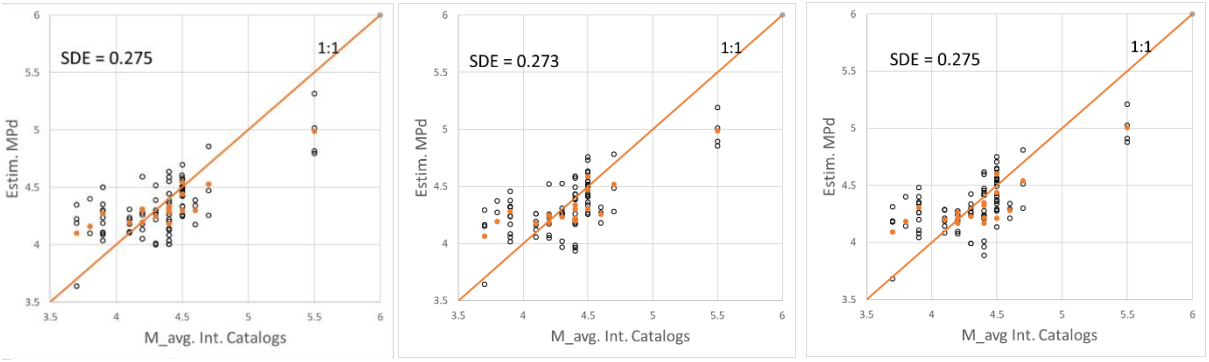

Figure 8. Best results of estimated magnitude M_{Pd} vs. average magnitude of international catalogs with 5 s HPF. a) broadband + short-period data without correction with 4 s time window, b) after correcting short-period, and c) the same as b) except for 3 s time-window.

We studied P_d for both broadband and short-period seismograms, with or without correction for the short-period (Figure 8 (a); (b)). There was only a small enhancement but this enhancement might have been increased if we had a large earthquake (M6.0 or higher) which would have caused P_d values to saturate much in short-period seismograms. All the used data had a limited epicentral distance up to 200 km. Using the same previous procedure of comparing results in case of using local catalog magnitude vs. using the average of international catalogs' magnitude. Again, the average international magnitude was more consistent. The improvement due to using 4 instead of 3 s time-window was insignificant in all cases (in the order of 0.001 of SDE) as shown in Figure 8 (b) and (c). The 4 s time window, as expected, gave a slightly better results, because the longer time window would allow more phases of the P-wave. The best combination was also with 5 s HPF and 4 s time-window, and in this case the best linear regression relation (in Figure 8 (b)) is:

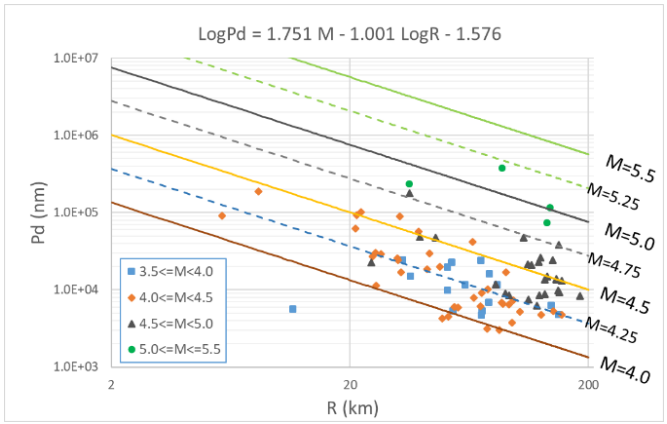

Figure 9. Scaling between P_d (nm) and R (km) for different magnitude ranges with different colors. The straight lines represent the obtained best fit relationship in Eq. (3) at selected magnitudes M.

$$M = 0.9 + 0.571 \times log\, P_d + 0.571 \times log\, R \qquad (3)$$

which in this case a multi-variable regression between magnitude and both log(P_d) in nm and log(R) in km where R is the epicentral distance, as shown in Figure 9. The results suggest that P_d is the best parameters with the least standard error. The drawback of using P_d is obviously the need of knowing R which mean that estimated magnitude would be dependent on the estimated epicentral location, i.e., wrong location would result in wrong magnitude estimation.

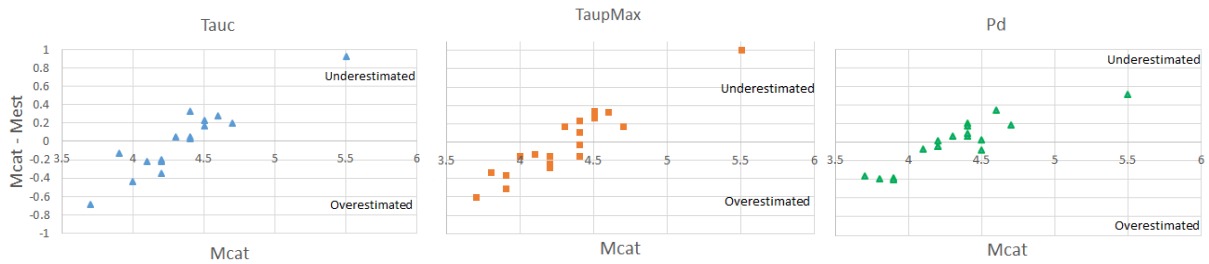

Figure 10. The error in estimation vs. magnitude for τ_c, τ_{max}^{p} and P_d. M_{Pd} has the smallest range of error in magnitude estimation ($-0.4 \leq Error \leq 0.5$).

Comparing the results of the three parameters, in Figure 10, we can see that the range of error in estimation is the least using P_d.

5. CONCLUSIONS

As the results suggested, initial peak displacement P_d has the strongest relation with the magnitude, while τ_c or τ_{max}^p could still be used for different purpose, like picking or filtering out teleseismic events. Although magnitude estimation from τ_{max}^p does not require the knowledge epicentral distance, limited epicentral distance still needed before calculating τ_{max}^p.

Results also suggest that simplified Instrumental correction can be used with short-period seismograms, in case of P_d and τ_{max}^p, Although the enhancement in results by the correction of short-period was small, it could have a higher enhancement in case of a range magnitude earthquake. The analysis of data indicated that the ENSN catalog of local magnitudes should be reviewed and unified. The best filter cut-off frequency was 5 s (0.2 Hz) in all the techniques tested, but this also would depend on the range of magnitudes of the analyzed dataset. If the dataset had included a M6.0 earthquake, it might have needed a filter with a longer cut-off period than 5 s. Also, the difference between 3 and 4 s time-window was insignificant. Therefore, the choice of the time-window between 3 and 4 s depends on the desired target time of computation (small effect on the estimation accuracy).

6. RECOMMENDATIONS

The limitations of the data available indicate the need for more stations in the target area, especially along the Red Sea shore near to the active faults. New stations should be established with 20 or 30 km of spacing. Strong-motion sensors can be used, which is a cheaper choice than broadband seismometers and do not require special treatment in station construction as broadband.

This study could be enhanced in case of larger magnitude events, ≥ M6.0, included in the future. Also, different studies should be conducted in other EEW subjects, such as automatic picking, automatic location and prediction of the seismic intensity. The EEW system software could be developed using open source platform, such as Earthworm automatic earthquake analysis software that is currently operated in the Egyptian National Seismic Network.

ACKNOWLEDGEMENTS

I would like to express my gratitude to my supervisors Dr. Bunichiro Shibazaki for his continuous support and valuable suggestions. Also, a debt of gratitude is owed to Dr. Masumi Yamada for providing her program and her expert advice.

REFERENCES

Allen R.V., 1978, Bull. seism. Soc. Am. 68, 1521–1532.
Allen, R.M., and Kanamori, H., 2003, Science, 300, 786-789.
Kanamori, H., 2005, Annu. Rev. Earth Planet. Sci., 33, 195-214.
Katsumata, A., 2008, JMA Quarterly Journal of Seismology, 71, 89-91.
Shieh, J.T., Wu, Y.M., and Allen, R.M., 2008, Geophysical Research Letters, 35.
Takanami, T., and Kitagawa, G., 1988, J. Phys. Earth, 36, 267–290.
Yamada, M., and Mori, J., 2009, Journal of Geophysical Research: Solid Earth, 114.
Yamada, M., Tamaribuchi, K., and Wu, S., 2014, J. Jpn. Assoc. Earthq. Eng, 14, 21-34.
Zhu, L., 2003, Geophysical Research Letters, 30.